Rock Mech Rock Eng (2016) 49:611–619
DOI 10.1007/s00603-015-0747-5

TECHNICAL NOTE

A 3D Fracture Network Model for the Undisturbed Rock Mass at the Songta Dam Site Based on Small Samples

Xudong Han[1] · Jianping Chen[1] · Qing Wang[1] · Yanyan Li[1] · Wen Zhang[1] · Tianwen Yu[1]

Received: 3 December 2014 / Accepted: 30 March 2015 / Published online: 12 April 2015

Keywords Rock mass · 3D fracture network model · Probability model · Small sample

List of symbols

w	Width of the sampling window
h	Height of the sampling window
α_i	Dip direction of the *i*th joint
α_r	Strike of the sampling window
θ_i	Dip angle of the *i*th joint
d_i	Fracture diameter of the *i*th joint
W_i	Weight formula for the *i*th joint
Rf_i	Corrected relative frequency of the *i*th joint
n	Number of joints in a fracture set
ε_i	The *i*th parameter of the supposed probability density function
l_j	The *j*th trace length of the measured joint of a fracture set
v	Sample size or number of sectors
S	Statistic of the Kolmogorov–Smirnov test
S^*	Critical value of the Kolmogorov–Smirnov test
p	Approximate significance level
μ_m	Mean trace length
σ_m	Standard deviation of the measured trace length distribution
μ_l	True mean trace length
σ_l	Standard deviation of the true trace length distribution
μ_D	Mean joint diameter
σ_D	Standard deviation of the joint diameter distribution
$(\mathrm{COV})_m$	Coefficient of variation of the measured trace length distribution
$E(D^m)$	The *m*th moment of the joint diameter, $m = 1$, 2, 3…
$E(l^m)$	The *m*th moment of the trace length, $m = 1$, 2, 3…
λ_i^1	Normal line density of the *i*th fracture set
λ_i^V	Fracture density in unit volume of the *i*th fracture set
V	Volume of simulated space region

✉ Jianping Chen
chenjpwq@126.com

[1] College of Construction Engineering, Jilin University, Changchun 130026, China

1 Introduction

Rock masses often contain discontinuities, which can be categorized as major discontinuities, such as faults and bedding plans that can be tens to hundreds of meters long, and minor discontinuities, such as joints and foliations with length varying from a few centimeters to tens of meters. Discontinuities endow a rock mass with discontinuous, inhomogeneous, and anisotropic features, and have an important influence on the mechanical and hydraulic behavior of the rock mass (Zhang et al. 2012; Li et al. 2014a, b). Thus, the characterization of rock fractures in terms of the orientation, spacing, size, aperture, etc. is a basic step for rock engineering design (Ivanova et al. 2014), and stochastic fracture network, also called discrete fracture network (DFN), models are deemed to be a suitable method for the characterization at present (Song and Lee 2001).

Various methods for generating DFN models have been developed (Jing 2003; Dershowitz et al. 2004; Dowd et al. 2007). It is recognized that a DFN model is mainly composed of three kinds of probability models, i.e., fracture occurrence probability distribution model, fracture size probability distribution model, and fracture location probability distribution model (Chen et al. 1995; Rafiee and Vinches 2008; Dowd et al. 2009; Xu and Dowd 2010; Ivanova et al. 2014).

In the fracture probability distribution model, the Fisher distribution, Bingham distribution, bivariate normal distribution, and the empirical probability distribution are widely used to describe the fracture orientations (Bingham 1964; Tian and Wan 1989; Chen et al. 1995; Marcotte and Henry 2002; Xu et al. 2013). In theory, the distribution that best fits the fracture orientation data can be determined by some statistical tests, such as the Kolmogorov–Smirnov (KS) test, Chi-square test, etc. (Zhang et al. 2013). However, due to measurement errors, natural variations in orientation, and the complexity of geological formations (Munier 2004), determining the optimum distribution for fracture orientations in a rock mass is difficult. In practice, the Fisher distribution and the empirical distribution have the most common use in describing the fracture orientation data not only because both distributions fit well with the distribution of fracture data, but also because they are easy to work with in terms of the mathematics (Tian and Wan 1989; Kemeny and Post 2003).

Research on estimating the fracture size distribution has turned to stereology, with the aim to use the available (or measured) fracture trace length probability distribution to obtain the required fracture size distribution (Tonon and Chen 2007). A stereological relationship between the true fracture trace length distribution and the fracture size distribution has been proposed by Warburton (1980), which can deal with the determination of 3D fracture structures from 2D data (Gorenflo and Vessella 1991; Tonon and Chen 2007). As can be seen from the relationship, the true trace length distribution of fractures should first be obtained before gaining the fracture size distribution. However, the available (or measured) trace length data are often collected in some finite zones, such as rock outcrops and exploration tunnels, which suffers from two major problems: the presence of sampling biases and the statistical difference between the measured trace length distribution and the true trace length distribution (Mauldon 1998; Zhang and Einstein 1998; Riley 2005; Tonon and Chen 2007; Li et al. 2014a, b). Several methods for correcting the sampling biases have been developed (Kulatilake and Wu 1984a; Zhang and Einstein 1998; Mauldon et al. 2001). The variance of the true trace length distribution can be inferred by the method introduced by Zhang (1999), who found that the coefficient of variation of the measured trace length distribution is always close to that of the true trace length distribution over a wide range of sampling window areas. However, the form of the true trace length distribution is unknown. It is usually assumed that the true trace lengths have the same distribution form as the measured trace lengths at present (Kulatilake et al. 1993; Zhang and Einstein 2000).

Fracture location, which is an important parameter of the DFN model, is usually modeled separately from the two above-mentioned fracture parameters (Xu and Dowd 2010), and the Poisson model is often used to describe the fracture location (Ross 1997; Min et al. 2004; Xu and Dowd 2010).

In addition, before generating a DFN model, the fracture data should first be separated into clusters because fracture sets may be hierarchical or independent, as defined by their geologic settings (Xu and Dowd 2010; Ivanova et al. 2014).

In this paper, the joint data collected from a tunnel at the Songta dam site were separated into three clusters by the fuzzy *K*-means algorithm (Hammah and Curran 1999, 2000). The empirical distribution was used to describe the fracture orientations in each cluster. An estimation method called the maximum likelihood with goodness-of-fit test was used to evaluate the parameter of the probability density function associated with the joint trace length data. It is more efficient than the method of moments with goodness-of-fit test technique, especially for small and moderate sample sizes (Bai et al. 1991; Rajan et al. 2014; Yilmaz and Sazak 2014). The KS test was adopted to determine the optimum measured trace length probability distribution for each fracture set. Compared with the Chi-square test, the KS test can be more effective for small sample data sets (Chen et al. 1995; Zhang et al. 2013). Analytical relations on estimating the distribution of fracture size from the distribution of trace length were gained according to the stereological relationship and the *m*th moment of the trace length when the joint shape was considered as a disk (Zhang and Einstein 2000; Tonon and Chen 2007). Finally, the 125 generated models were tested by comparing them with the field data, and the test results showed that the method of modeling a 3D fracture network is suitable for samples with small sizes.

2 Data Acquisition

The investigated rock mass is located at the dam site area of the Songta hydropower station under construction, which lies on the upper reaches of Nu River in south-west China. The flow direction of Nu River in the dam site area is approximately 188°SW, and the elevation of the normal water level is 1700 m.

A concrete double-cured arch dam is designed for this project, with a maximum height of 318 m. It will be one of the highest arch dams in the world. The normal storage water level elevation will be 1925 m and the total storage capacity will reach 4.55 billion m^3. The Songta hydropower station will have a hydroelectric generating capacity of 3600 MW.

The Gebu-Songta fault located north-east of the dam site passes with a minimum distance of 2.5 km (Li et al. 2014a, b). In addition, no regional fault lies in the dam area.

Two forms of lithology from the late Yanshanian (Cretaceous) period are exposed in the dam site area. The predominant lithology is biotite granite, which is mainly composed of quartz, plagioclase, potassium feldspar, and biotite. Moreover, affected by tectonism, the biotite granite has been slightly metamorphosed, with a cataclastic texture characterized by the fragmentation of the feldspar phenocrysts (Chen et al. 2013; Li et al. 2014a, b). The other lithology is plagioclase amphibolite outcropping as dykes, with widths varying from 0.05 to 5 m. In the contact zone of the two forms of lithology, the plagioclase amphibolite has experienced mineral alteration. Moreover, according to field investigation, the aperture of most joints is very small.

The size of the underground excavation tunnel is about 200 m long, 2 m wide, and 2 m high. The investigated rock mass along the tunnel was divided into three regions according to the effect degree of unloading and weathering: strongly disturbed zone, weakly disturbed zone, and undisturbed zone. Data collection was undertaken using the window sampling method and the fractures within the downstream wall of the tunnel with trace lengths longer than 0.5 m were measured (Li et al. 2014a, b). In this study, a relatively homogenous rock mass of length 80 m in the undisturbed zone was selected for a case study, where a total of 128 fractures were mapped. Fracture information, including the terminal point coordinate, the dip direction, and the dip angle, were collected using a rectangular sampling window of dimensions 80 m long and 1.8 m high (Fig. 1).

Based on fracture orientations, the joints were separated into clusters using the fuzzy K-means algorithm introduced by Hammah and Curran (1999), and the optimal number of clusters was determined by minimizing an objective function called the Xie-Beni index (Hammah and Curran 2000). The clustering results are shown in Table 1 and Fig. 2.

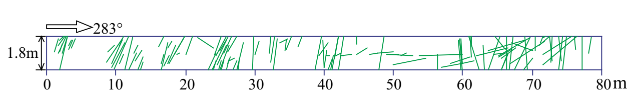

Fig. 1 Distributions of joint traces within the downstream wall of the tunnel

3 Fracture Occurrence Probability Distribution Model

In this study, the empirical probability distribution was used to describe the fracture orientation for each fracture set. Due to sampling bias on the orientation of discontinuities (Kulatilake and Wu 1984b; Chen et al. 1995; Tonon and Chen 2007; Wu et al. 2011), the relative frequency of measured joint orientations of each set should be corrected before generating the 3D fracture network, and it can be calculated as given below.

The mathematic weights of each joint in a fracture set was first calculated (Kulatilake and Wu 1984b; Chen et al. 1995), and when the joint data are collected with a vertical sampling window, the weight formula W_i is described as:

$$W_i = \{whd_i[\cos^2\theta_i + \sin^2\theta_i\cos^2(\alpha_r - \alpha_i)]^{0.5} + \cdots 0.25\pi d_i^2[w\sin\theta_i|\cos(\alpha_r - \alpha_i)|h\cos\theta_i]\}^{-1} \quad (1)$$

Then, the corrected relative frequency Rf_i can be obtained based on Eq. (1):

$$\mathrm{Rf}_i = \frac{W_i}{\sum_{i=1}^{n} W_i} \quad (2)$$

Due to the absence of the diameter values d_i for joints in simulating the 3D fracture network, the mean diameter value was used for all the discontinuities (Kulatilake and Wu 1984b; Chen et al. 1995).

In order to describe the discrete characteristics of joint data in each cluster, the values of the Fisher constant and the spherical standard variance in the semi-spherical coordinate system were adopted in this paper, as shown in Table 1 (Tian and Wan 1989; Chen et al. 1995; Min et al. 2004).

4 Fracture Size Probability Distribution Model

4.1 Calculation of the Parameters of the Measured Trace Length Distribution

In this research, the maximum likelihood estimation algorithm was used to deduce the probability distribution of the measured trace length data of each fracture set. The algorithm is described as follows:

1. Assume the joint trace length probability distribution type.
2. Obtain the likelihood function $L(\varepsilon_1,\ldots\varepsilon_i)$ or logarithmic likelihood function $\ln L(\varepsilon_1,\ldots\varepsilon_i)$ of the measured traces length data according to the above supposed distribution:

Table 1 Modeling parameters of the observed data

Fracture set	Fracture number	Mean pole direction (°)	Mean dip angle (°)	Fisher constant	Spherical std. (°)	Trace length				
						Measured		Corrected		Distribution form
						Mean (m)	Std. (m)	Mea (m)	Std. (m)	
1	74	113.3	48.3	17.11	10.01	1.35	0.79	3.76	2.19	Log-normal
2	35	100.6	11.8	28.40	8.75	2.19	1.57	2.65	1.90	Gamma
3	19	265.0	82.2	10.87	14.43	1.48	0.57	2.97	1.15	Log-normal

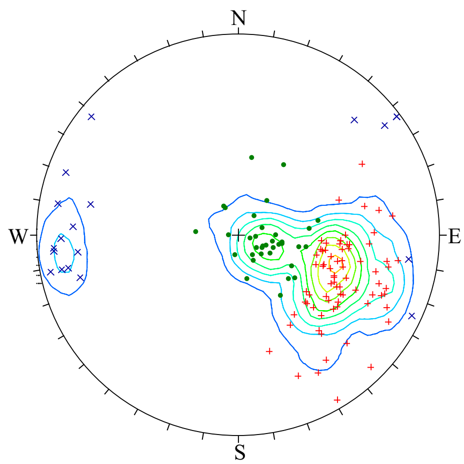

Fig. 2 Equal-area projection diagram for the three fracture sets

$$L(\varepsilon_1,\ldots\varepsilon_i)=\prod_{j=1}^{n} f(l_j,\varepsilon_1,\ldots\varepsilon_i) \tag{3}$$

or:

$$\ln L(\varepsilon_1,\ldots\,\varepsilon_i)=\prod_{j=1}^{n}\ln f(l_j,\varepsilon_1,\ldots\varepsilon_i) \tag{4}$$

where $f(l_j,\varepsilon_1,\ldots\,\varepsilon_i)$ denotes the supposed probability density function.

3. Solve the likelihood equation or logarithmic likelihood equation:

$$\frac{\partial L(\varepsilon_1,\ldots\,\varepsilon_i)}{\partial\varepsilon_i}=0 \tag{5}$$

or:

$$\frac{\partial \ln L(\varepsilon_1,\ldots\,\varepsilon_i)}{\partial\varepsilon_i}=0 \tag{6}$$

4. Determine the parameter values $\varepsilon_1,\ldots\varepsilon_i$ of the assumed probability density function associated with the measured trace length data.

According to aforementioned process, the parameters of five common probability density distributions, including the log-normal distribution, exponential distribution, normal distribution, gamma distribution, and uniform distribution (Zhang and Einstein 2000; Tonon and Chen 2007), can be obtained.

4.2 Kolmogorov–Smirnov Test

The KS test is a nonparametric test whose statistical procedure does not rely on assumptions about the form of the distribution of populations (Johnson and Bhattacharyya 2009). In this study, the KS test was adopted to examine whether the difference between the above-mentioned distributions of measured trace length and the sample data is significant. The statistic S, named the KS test distance, is defined by (Wei 1989; Drew et al. 2000):

$$S=\max|F(l)-S_v(l)| \tag{7}$$

where $S_v(l)$ indicates the cumulative distribution of the sample data, which is also called the empirical distribution function (see Table 2), and $F(l)$ denotes the cumulative distribution of the measured trace length data.

Using an approximation, the approximate significance level p for the critical value $S*$ of the KS distribution at a specified significance level is described as (Wei 1989; Zhang et al. 2012; Li et al. 2014a, b):

$$p(S\geq S*)=2\sum_{i=1}^{\infty}(-1)^{i-1}\exp[-2i^2S^2(\sqrt{n}+0.12+0.11\sqrt{n})^2] \tag{8}$$

In this study, the significance level is set to 0.05 (Zhang et al. 2012 and Li et al. 2014a, b). When the statistic S of a distribution is smaller than the critical value $S*$ at the significance level, the distribution of trace length data can be accepted. When the statistic S of one distribution among accepted distributions is the smallest, the distribution is considered as the optimum distribution for the measured trace length. Based on the KS test, the optimum distribution of each fracture set was determined, and the mean trace length μ_m and standard deviation σ_m of the optimum distribution for the measured trace length data of each cluster are also calculated (see Table 1). As an illustration, the comparison between the optimum distribution and the empirical distribution of the first cluster is shown in Fig. 3.

Table 2 The procedure to calculate the empirical distribution of sparse data

Sectors	Frequency number	Probability value	Cumulative probability value
(l_1, l_2)	n_1	$n_1/\Delta l$	$n_1/\Delta l$
(l_2, l_3)	n_2	$n_2/\Delta l$	$n_1/\Delta l + n_2/\Delta l$
…	…	…	…
(l_{n-1}, l_n)	n_{n-1}	$n_{n-1}/\Delta l$	$n_1/\Delta l + n_2/\Delta l + \cdots + n_{n-1}/\Delta l$
(l_n, ∞)	n_n	$n_n/\Delta l$	1

Note: $\Delta l = l_2 - l_1 = l_3 - l_2 = \cdots = l_n - l_{n-1}$

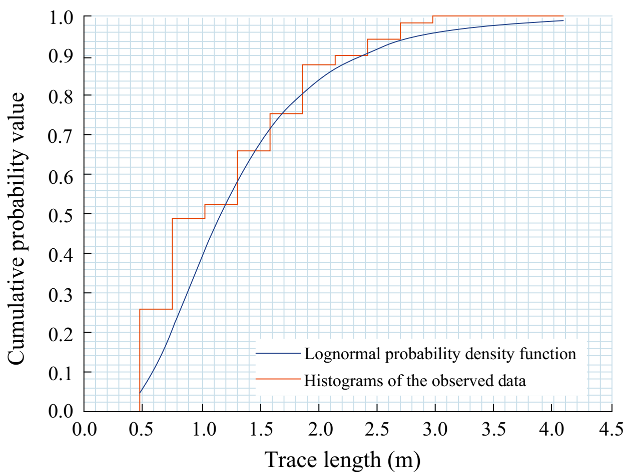

Fig. 3 The Kolmogorov–Smirnov (KS) goodness-of-fit test for the observed data

4.3 Estimation of the Fracture Size Distribution from the Trace Length Distribution

The general stereological relationship between the true trace length distribution and the discontinuity size distribution proposed by Warburton (1980) was used to infer the discontinuity size distribution. The mean trace length μ_l of the true trace length distribution can be obtained using the method introduced by Kulatilake and Wu (1984a). The coefficient of variation of the true trace length distribution was considered as the same as that of the measured trace length distribution (Zhang and Einstein 2000). For sampling in rectangular windows, when the discontinuity type is considered as a disk, the process of estimating the diameter distribution is performed in the following steps:

1. Calculate the true mean trace length μ_l(Kulatilake and Wu 1984a).
2. Compute the standard deviation σ_l:

$$\sigma_l = \mu_l (\mathrm{COV})_m \tag{9}$$

3. Estimate the fracture diameter distribution from the true trace length distribution based on Warburton's equation and the mth moment of the trace length (Zhang and Einstein 2000; Tonon and Chen 2007). The procedure of obtaining the fracture diameter distribution from the true trace length distribution is described as follows:

   (a) Assume a joint diameter distribution;
   (b) The mean diameter μ_D and the standard deviation σ_D of the assumed joint diameter distribution is estimated by:

$$u_l = \frac{\pi[(\mu_D)^2 + (\sigma_D)^2]}{4\mu_D} \tag{10}$$

   and:

$$[(\mu_l)^2 + (\sigma_l)^2] = \frac{2E(D^3)}{3\mu_D} \tag{11}$$

   (c) Check the assumed fracture diameter distribution using the following equation:

$$\frac{E(D^4)}{E(D^2)} = \frac{4}{3}\frac{E(l^3)}{E(l)} \tag{12}$$

Table 3 Derived distribution of $g(D)$

Fracture set	Assumed distribution form of $g(D)$	μ_D	σ_D	$E(D)^4/E(D)^2$	$4E(l^3)/3E(l)$	Recommended distribution form for $g(D)$
1	Log-normal	3.86	1.89	43.61	45.28	Log-normal
	Exponential	2.39	2.39	68.76		
	Gamma	3.64	2.04	41.99		
2	Log-normal	2.41	1.53	31.30	28.76	Gamma
	Exponential	1.69	1.69	34.15		
	Gamma	2.02	1.65	28.74		
3	Log-normal	3.55	0.90	17.23	17.88	Log-normal
	Exponential	1.89	1.89	42.90		
	Gamma	3.54	0.93	17.16		

Table 4 Density and quantity of simulated fracture disks

Fracture set	Normal line density	Volume density	Fracture number
1	0.89819	0.0619106	22,288
2	0.85507	0.1600338	57,612
3	0.31967	0.0303451	10,924

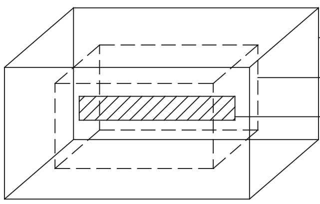

Fig. 4 Graphical representation of the relationship among the simulation space, generated model, and sampling window

If the left and right sides of Eq. (12) are the closest to each other, then the assumed fracture diameter distribution is the optimum.

In this study, three common probability distributions, including the exponential distribution, log-normal distribution, and gamma distribution (Zhang and Einstein 2000; Tonon and Chen 2007), were selected to find a suitable diameter distribution for each fracture set. By assuming the three distribution forms for each fracture set, the optimum diameter probability distribution of each fracture set can be determined with the above process of estimating the diameter distribution (see Table 3).

5 Fracture Location Probability Distribution Model

The 2D joint spacing information is often used to deduce the 3D joint spacing information (Zhang et al. 2013). The 2D joint spacing information in some finite zones, such as rock outcrops and exploration tunnels, can be obtained by arranging a series of scanlines in the sampling window (Chen et al. 2004), and the normal spacing information of each fracture set can be calculated according to the 2D joint spacing information by the method introduced by Karzulovic and Goodman (1985). When the shape of the joint is considered as a disk and the disk center is deemed to follow the homogeneous Poisson distribution in the simulated rock mass, the volume density λ_i^V of each fracture set can be deduced by the normal line density λ_i^1 with the following equation (Kulatilake et al. 1993; Oda 1982):

$$\lambda_i^V = \frac{4\lambda_i^1}{\pi E(D^2)} \tag{13}$$

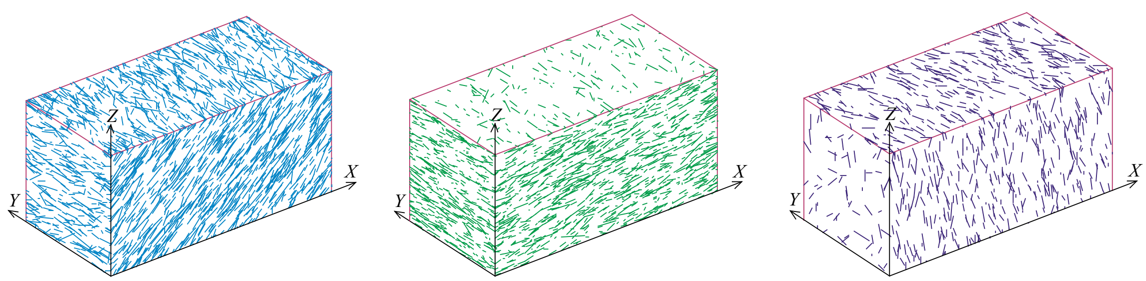

Fig. 5 3D illustrations of the fracture sets: **a** set 1, **b** set 2, **c** set 3

Table 5 Comparison between the generated model and the field data

Fracture set	Field/generated	Mean pole dip (°)	Mean dip angle (°)	Fisher constant	Spherical std. (°)	Measured trace length		Corrected trace length (m)	Volume density (m^{-3})	Fracture number
						Mean (m)	Std. (m)			
1	Field	113.3	48.3	17.11	10.01	1.35	0.79	3.76	0.062	74
	Generated	112.1	45.3	26.54	9.85	1.65	0.75	3.79	0.062	73
2	Field	100.6	11.8	28.40	8.75	2.19	1.57	2.65	0.160	35
	Generated	89.8	8.0	27.66	9.88	2.47	1.76	2.58	0.160	34
3	Field	265.0	82.0	10.87	14.43	1.48	0.57	2.97	0.030	19
	Generated	272.5	79.0	14.36	13.08	1.26	0.51	2.80	0.030	20

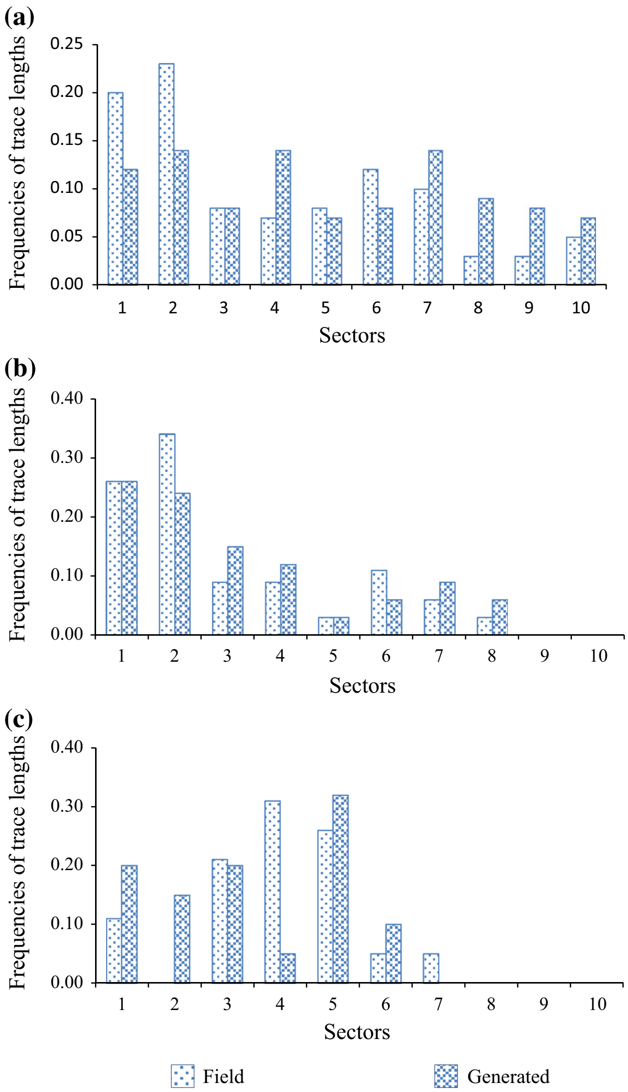

Fig. 6 Comparisons between the generated trace lengths and the field trace length data for the fracture sets: **a** set 1, **b** set 2, **c** set 3

Based on Eq. (14), the number n_i of joint disks in the simulated space region for the ith fracture set is:

$$n_i = V\lambda_i^v \tag{14}$$

5.1 3D Fracture Network Simulation and Model Test

As required by the project simulation, the size of the 3D fracture network was designed as 80 m × 40 m × 40 m. In order to remove the edge effect of the generated model, the simulation space region was set as 100 m × 60 m × 60 m (Zhang et al. 2013). When the size of the simulation space region was determined, the number of simulated joints for each fracture set can be obtained according to Eqs. (13) and (14) (see Table 4), and then the Monte Carlo simulation was applied to simulate the 3D fracture network model including the fracture occurrence probability distribution model, fracture size probability distribution model, and fracture location probability distribution model in the simulation space region by using the Poisson process (Chen et al. 1995). The three kinds of probability distribution models were simulated five times, respectively. Finally, a total of 125 3D fracture network models were taken from the simulation space (see Fig. 4).

In order to check the generated models based on the above-mentioned modeling method, an arranged sampling window that has the same size as that in the field survey was set to cut the simulated rock mass for obtaining the simulated joints information, and it should also be parallel to the actual sampling window so that the obtained simulation joint data can be compared with the field fractures. The compared parameters include the mean pole direction and dip angle, the Fisher constant and the spherical standard variance of joint orientations, the measured mean trace length and the standard deviation, the corrected mean trace length, the volume density, and the number of fractures in the two sampling windows. By the comparison of these parameters between the generated models and the field data, the optimum model among these generated models can be obtained (see Fig. 5). The results of the comparison between the selected model and the field data are shown in Table 5, and the comparisons of the trace lengths, the fracture orientations, and the trace maps are shown in Figs. 6, 7, and 8, respectively.

6 Conclusion

This paper presents a method for modeling 3D fracture networks in a rock mass which can obtain a satisfactory simulation result for small samples.

In this method, the empirical probability distribution was used to describe the fracture orientations; this distribution type fits well with the distribution of the fracture data collected from field surveys and it is easy to carry out mathematically. The maximum likelihood estimation algorithm and the Kolmogorov–Smirnov (KS) test were used to determine the optimum probability distribution for the measured trace length data. When the discontinuity is considered as a disk, the fracture diameter distribution of each cluster was calculated though certain analytical relations between the fracture diameter distribution and the true trace length distribution, which can be obtained on the basis of the measured trace length. In consideration of the characteristics of the rock mass simulated, a homogeneous Poisson model was used to described the relatively homogeneous rock mass region, which is undisturbed by unloading and weathering.

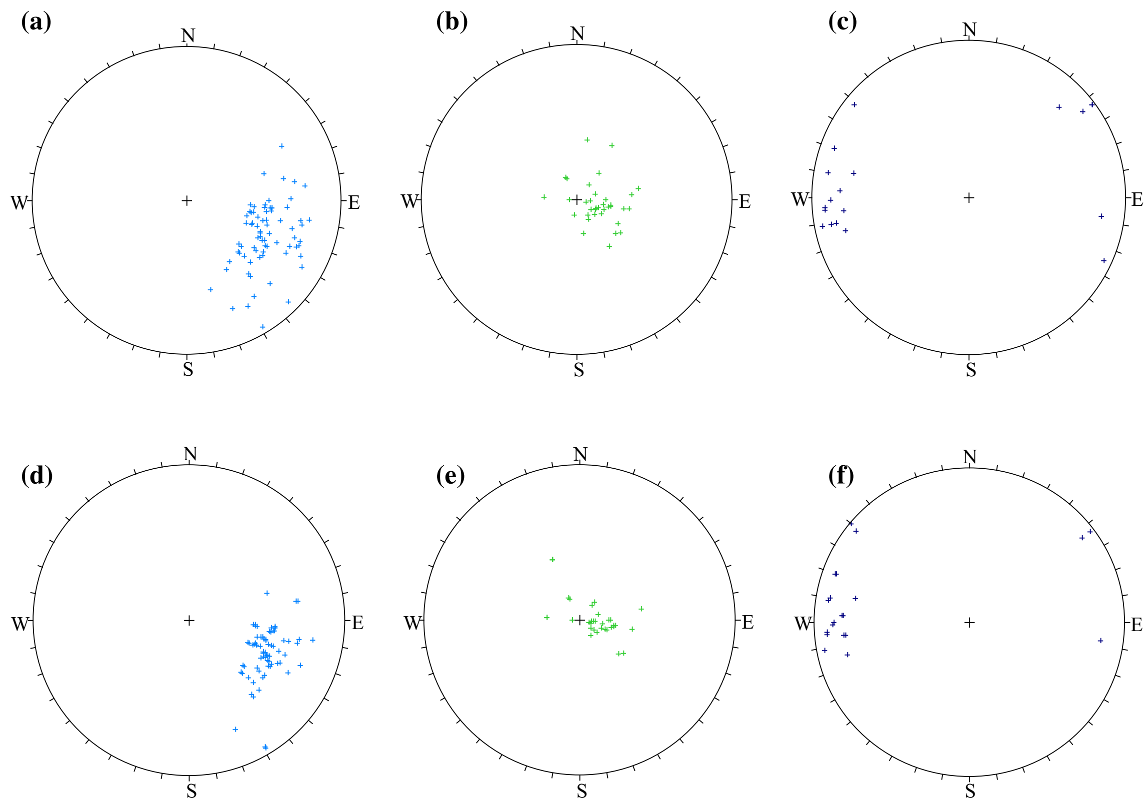

Fig. 7 Comparisons between the generated fracture orientations and the field data for the fracture sets. Field: **a** set 1, **b** set 2, **c** set 3. Predicted: **d** set 1, **e** set 2, **f** set 3

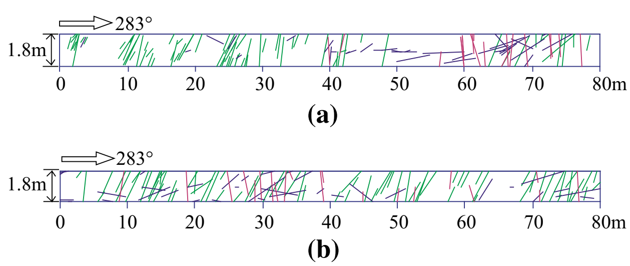

Fig. 8 Comparisons between the measured trace maps and the simulated trace maps (*green lines* set 1, *red lines* set 2, *blue lines* set 3): **a** the measured trace maps, **b** the simulated trace maps (color figure online)

Based on the method, a suitable 3D fracture network model for the rock mass at the Songta dam site was obtained. Through the model test, the method of building a 3D fracture network for the rock mass based on small samples was satisfying. Further work, such as calculating the 3D connectivity of rock mass and creating a block system based on the 3D fracture network, can be done on the basis of the model.

Finally, it should be noted that, due to the limit in size of the underground excavation tunnel, the fracture information was collected with a narrow sampling window whose width and height were 80 and 1.8 m, respectively. This meant that much larger fractures could not be measured completely and produced larger deviations between the estimated trace length and the true length (Li et al. 2011). Though the fracture information was collected from the undisturbed rock mass and the trace lengths were relatively small in this study, a larger deviation still existed because of the height of the sampling window being too small. We thank the comment proposed by our reviewer that the very small fractures do not really represent the in situ conditions.

Acknowledgments This work was supported by the State Key Program of the National Natural Science Fund of China (Grant No. 41330636), the National Natural Science Fund of China (Grant Nos. 41402242, 41402243, and 41202197), and Graduate Innovation Fund of Jilin University (Grant No. 2014062). We thank Dr. Giovanni Barla and an anonymous reviewer for the excellent reviews that helped to improve the manuscript.

References

Bai J, Jakeman AJ, McAleer M (1991) A new approach to maximum likelihood estimation of the three-parameter gamma and Weibull distributions. Aust J Stat 33:397–410

Bingham C (1964) Distributions on the sphere and on the projective plane. PhD thesis, Yale University, New Haven, CT

Chen JP, Xiao SF, Wang Q (1995) Three dimensional network modeling of stochastic fractures. Northeast Normal University Press, Changchun
Chen JP, Wang Q, Zhao HL (2004) Obtaining RQD of rock mass by sampling window method. Chin J Rock Mech Eng 23:1491–1495
Chen MX, Chen BG, Shen SH (2013) Application of drilling deviation correcting and deflecting techniques in geological exploration at Songta Hydropower Station. Rock Soil Drill Tunn 40:35–38
Dershowitz WS, La Pointe PR, Doe TW (2004) Advances in discrete fracture network modeling. In: Proceedings of the US EPA/NGWA fractured rock conference, Portland, ME, September 2004, pp 882–894
Dowd PA, Xu C, Mardia KV, Fowell RJ (2007) A comparison of methods for the stochastic simulation of rock fractures. Math Geol 39:697–714
Dowd PA, Martin JA, Xu C, Fowell RJ, Mardia KV (2009) A three-dimensional fracture network data set for a block of granite. Int J Rock Mech Min Sci 46:811–818
Drew JH, Glen AG, Leemis LM (2000) Computing the cumulative distribution function of the Kolmogorov–Smirnov statistic. Comput Stat Data Anal 34:1–15
Gorenflo R, Vessella S (1991) Abel integral equations: analysis and applications. Springer, Berlin
Hammah RE, Curran JH (1999) On distance measures for the fuzzy K-means algorithm for joint data. Rock Mech Rock Eng 32:1–27
Hammah RE, Curran JH (2000) Validity measures for the fuzzy cluster analysis of orientations. IEEE Trans Pattern Anal Mach Intell 22:1467–1472
Ivanova VM, Sousa R, Murrihy B, Einstein HH (2014) Mathematical algorithm development and parametric studies with the GEOFRAC three-dimensional stochastic model of natural rock fracture systems. Comput Geosci 67:100–109
Jing L (2003) A review of techniques, advances and outstanding issues in numerical modelling for rock mechanics and rock engineering. Int J Rock Mech Min Sci 40:283–353
Johnson RA, Bhattacharyya GK (2009) Statistics: principles and methods, 6th edn. Wiley, Hoboken
Karzulovic A, Goodman RE (1985) Determination of principal joint frequencies. Int J Rock Mech Min Sci Geomech Abstr 22:471–473
Kemeny J, Post R (2003) Estimating three-dimensional rock discontinuity orientation from digital images of fracture traces. Comput Geosci 29:65–77
Kulatilake PHSW, Wu TH (1984a) Estimation of mean trace length of discontinuities. Rock Mech Rock Eng 17:215–232
Kulatilake PHSW, Wu TH (1984b) Sampling bias on orientation of discontinuities. Rock Mech Rock Eng 17:243–253
Kulatilake PHSW, Wathugala DN, Stephansson OVE (1993) Stochastic three dimensional joint size, intensity and system modelling and a validation to an area in Stripa Mine, Sweden. Soils Found 33:55–70
Li XZ, Zhou YY, Wang ZT, Zhang YS, Guo L, Wang YZ (2011) Effects of measurement range on estimation of trace length of discontinuities. Chin J Rock Mech Eng 30:2049–2056
Li XJ, Zuo YL, Zhuang XY, Zhu HH (2014a) Estimation of fracture trace length distributions using probability weighted moments and L-moments. Eng Geol 168:69–85
Li YY, Wang Q, Chen JP, Han LL, Song SY (2014b) Identification of structural domain boundaries at the Songta dam site based on nonparametric tests. Int J Rock Mech Min Sci 70:177–184
Marcotte D, Henry E (2002) Automatic joint set clustering using a mixture of bivariate normal distributions. Int J Rock Mech Min Sci 39:323–334
Mauldon M (1998) Estimating mean fracture trace length and density from observations in convex windows. Rock Mech Rock Eng 31:201–216
Mauldon M, Dunne WM, Rohrbaugh MB (2001) Circular scanlines and circular windows: new tools for characterizing the geometry of fracture traces. J Struct Geol 23:247–258
Min KB, Jing L, Stephansson O (2004) Determining the equivalent permeability tensor for fractured rock masses using a stochastic REV approach: method and application to the field data from Sellafield, UK. Hydrogeol J 12:497–510
Munier R (2004) Statistical analysis of fracture data, adapted for modelling discrete fracture networks—version 2. Swedish Nuclear Fuel and Waste Management Company, Stockholm
Oda M (1982) Fabric tensor for discontinuous geological materials. Soils Found 22:96–108
Rafiee A, Vinches M (2008) Application of geostatistical characteristics of rock mass fracture systems in 3D model generation. Int J Rock Mech Min Sci 45:644–652
Rajan J, den Dekker AJ, Sijbers J (2014) A new non-local maximum likelihood estimation method for Rician noise reduction in magnetic resonance images using the Kolmogorov–Smirnov test. Signal Proc 103:16–23
Riley MS (2005) Fracture trace length and number distributions from fracture mapping. J Geophys Res 110:B08414
Ross SM (1997) Introduction to probability models, 6th edn. Academic Press, New York
Song JJ, Lee CI (2001) Estimation of joint length distribution using window sampling. Int J Rock Mech Min Sci 38:519–528
Tian KM, Wan L (1989) Study on permeability of anisotropic fracture medium. Academy Press, Beijing
Tonon F, Chen S (2007) Closed-form and numerical solutions for the probability distribution function of fracture diameters. Int J Rock Mech Min Sci 44:332–350
Warburton PM (1980) A stereological interpretation of joint trace data. Int J Rock Mech Min Sci Geomech Abstr 17:181–190
Wei ZS (1989) Course on probability and mathematical statistics. Higher Education Press, Beijing
Wu Q, Kulatilake PHSW, Tang HM (2011) Comparison of rock discontinuity mean trace length and density estimation methods using discontinuity data from an outcrop in Wenchuan area, China. Comput Geotech 38:258–268
Xu CS, Dowd P (2010) A new computer code for discrete fracture network modelling. Comput Geosci 36:292–301
Xu LM, Chen JP, Wang Q, Zhou FJ (2013) Fuzzy C-means cluster analysis based on mutative scale chaos optimization algorithm for the grouping of discontinuity sets. Rock Mech Rock Eng 46:189–198
Yilmaz H, Sazak HS (2014) Double-looped maximum likelihood estimation for the parameters of the generalized gamma distribution. Math Comput Simul 98:18–30
Zhang L (1999) Analysis and design of drilled shafts in rock. PhD thesis, Massachusetts Institute of Technology, Cambridge, MA
Zhang L, Einstein HH (1998) Estimating the mean trace length of rock discontinuities. Rock Mech Rock Eng 31:217–235
Zhang L, Einstein HH (2000) Estimating the intensity of rock discontinuities. Int J Rock Mech Min Sci 37:819–837
Zhang W, Chen JP, Liu C, Huang R, Li M, Zhang Y (2012) Determination of geometrical and structural representative volume elements at the Baihetan dam site. Rock Mech Rock Eng 45:409–419
Zhang W, Chen JP, Cao ZX, Wang RY (2013) Size effect of RQD and generalized representative volume elements: a case study on an underground excavation in Baihetan dam, Southwest China. Tunn Undergr Space Technol 35:89–98